JOURNAL OF GEOPHYSICAL RESEARCH VOL. 75, NO. 8, MARCH 10, 1970

Love Waves in Nonuniform Wave Guides: Finite Difference Calculations

DAVID M. BOORE

Department of Earth and Planetary Sciences
Massachusetts Institute of Technology, Cambridge, Massachusetts 02139

A simple finite difference approximation to the elastic equations of motion is successfully used to solve various wave-propagation problems possessing analytical solutions. On this basis the method is extended to the problem of Love waves propagating across an ocean-continent type boundary. Numerical propagation of an initial transient solution results in seismograms at various distances. The Fourier transforms of these seismograms are used to calculate phase velocity, group delay, and amplitude-transfer coefficients for various seismometer combinations across the transition region. Some results are: the transition zone can have a small but noticeable effect on phase velocities measured between stations situated away from the zone; a phase-velocity anisotropy exists for waves propagating in opposite directions across the same array. In general, waves propagating into the region of thinning have anomalously high-phase velocities and vice versa. This is especially noticeable for velocities measured over the zone of transition, where the perturbations of the phase velocity of continent-to-ocean waves from the expected local phase velocity can exceed the variations expected from the continent–ocean structural differences. The behavior at a distance from the boundary justifies the well-established method of calculating effective group velocities by means of inverse averages of regional group velocities and also indicates a simple correction for the effect of the ocean–continent boundary that can be applied to calculations of earthquake-source mechanisms based on the method of amplitude equalization.

INTRODUCTION AND SUMMARY

The effect of lateral inhomogeneities on surface-wave propagation is becoming increasingly important as seismologists study the structure of the earth in ever finer detail. Perturbations from such structural complexities can be viewed either as noise when the usual simplifying assumptions of homogeneous, plane-layered, perfectly elastic media are applied, or as observational quantities from which structural interpretations may be derived. In either case, it is important to have a method by which the theoretical effects of a given model can be computed. This paper describes such a method.

For several reasons the computations in this paper are limited to two-dimensional horizontal shear motion: (1) less storage space and computer time are required than in the corresponding vector-elastic computations, and thus more realistic heterogeneities can be modeled within the space-time limits available; (2) as opposed to Rayleigh waves [*Alexander*, 1963; *Kuo and Thompson*, 1963], model experiments involving Love waves are impractical, and thus a numerical model experiment must be used; (3) observations often indicate that Love waves are more sensitive to structural complexities than are Rayleigh waves. Although a sizeable literature exists on the approximate treatment of Love waves propagating in laterally heterogeneous structures [e.g., *Knopoff and Mal*, 1967; *Ghosh*, 1962], the assumptions made in these studies, usually stated in terms of the relative change of structure per wavelength, make the application of the results to realistic earth models of questionable value [*Boore*, 1969]. For this reason the straightforward numerical integration of the relevant boundary-value problem is attractive, especially since present digital computers can handle significant problems at reasonable cost.

In this paper a simple form of lateral heterogeneity is treated: a uniform layer of nonconstant thickness (but planar free surface) covering a homogeneous half-space. In particular, the heterogeneity is confined to a region connecting two quarter planes in each of which the layer has a constant thickness (Figure 1),

and can thus be thought of as a simplified model of the ocean–continent boundary. By studying the dispersion and amplitude-transfer coefficients for various station combinations across the transition region, several interesting features that have relevance to actual observations can be seen. Prominent among these features is the significant anisotropy which exists in the measured phase velocity of waves propagating in opposite directions across a given station array located over the transition region. Also of interest is the relative increase or decrease in the amplitudes of waves propagating across the region. This phenomenon is also anisotropic and is large enough in the particular model studied to be diagnostic of the underlying structure. Of importance to studies of earthquake-source mechanisms via the amplitude equalization of surface waves is the indication that, notwithstanding the complexities in the transition region, a simple correction can usually be applied for the influence of the boundary on the observed amplitudes. Although the above observations are based on a model of the ocean–continent transition, the technique can also be applied to calculations of the effect of local structure. Since seismometers are not placed conveniently with respect to the ocean–continent boundary, it is in the latter case that the technique can be most helpful. Application to measurements is now under way.

In the next section of the paper will be a statement of the relevant boundary-value problem, and in the section following the finite-difference formulation of the solution will be discussed. As a check of the method, the fourth section will be an application to problems possessing analytical solutions. With this as a background the solution of the originally posed problem, along with discussions of the seismological implications, will be given in the fifth section.

Statement of Problem

The formulation is that of a standard two-dimensional initial boundary-value problem. Consider the geometry in Figure 1, where a linear, isotropic, homogeneous (lih) material of rigidity μ_1, density ρ_1 and nonconstant thickness overlies a lih material with elastic constants μ_2, ρ_2. The interface between the two materials is in welded contact, and the upper

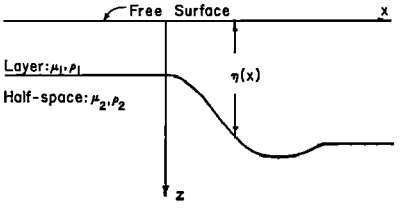

Fig. 1. Possible inhomogeneity that can be treated with the finite-difference method. The plane $z = 0$ is a stress-free surface; the two elastic materials are in welded contact at the interface $z = \eta\ (x)$.

surface is stress free. Let the thickness of the layer be $\eta(x)$. The mathematical description of the problem is:

Equations of motion:

$$(\partial^2 v_i/\partial t^2) = \beta_i{}^2 \nabla^2 v_i$$
$$\nabla^2 v_i = (\partial^2 v_i/\partial x^2) + (\partial^2 v_i/\partial z^2) \tag{1}$$
$$i = 1, 2$$

Boundary conditions:

$$(\partial v_1/\partial z)_{z=0} = 0 \tag{2}$$

$$\mu_1(\partial v_1/\partial n)_{z=\eta(x)} = \mu_2(\partial v_2/\partial n)_{z=\eta(x)} \tag{3}$$

$$(v_1)_{z=\eta(x)} = (v_2)_{z=\eta(x)} \tag{4}$$

Initial conditions:

$$(v)_{t=0} = f(x, z)$$
$$(\partial v/\partial t)_{t=0} = g(x, z) \tag{5}$$

where v_1, v_2 are the horizontal (y) displacements in media 1 and 2 respectively. The subscripts are for clarity and are omitted when not needed. β_1, β_2 are the shear velocities and are given by $\beta_i = (\mu_i/\rho_i)^{1/2}$. $\partial/\partial n$ corresponds to a derivative normal to the interface.

Although sources can be included quite easily in the formalism, the basic assumption in this paper is that we are dealing with well-formed, source-free Love waves that impinge on inhomogeneous, complicated structures. Because of the basic forward-step nature of wave propagation, this problem can be formulated quite easily. Note in Figure 1 that the thickness of the layer for $x < 0$ is constant. We assume that a transient disturbance has been set up by sources at infinity such that at the time $t = 0$ the wave

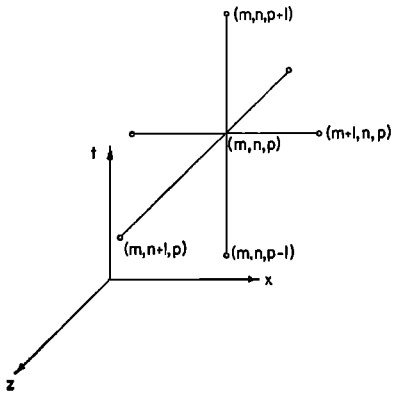

Fig. 2. A section of the discretized (x, z, t) space. Any point in the space is uniquely characterized by its x, z, and t indices m, n, and p. The seven points shown here are those used in the finite-difference approximation of the equation of wave motion discussed in the text. Note the uneven grid spacing with z.

motion is confined to the region $x < 0$ and is appropriate to a Love wave propagating on a layer of constant thickness over a half-space. Such a disturbance will completely satisfy the equations of motion and boundary conditions. With this as a starting condition, the system is turned loose and the transient disturbance is propagated into the inhomogeneous region. This is accomplished by employing a finite-difference approximation to the problem.

Finite-Difference Formulation

Although finite-difference techniques have been in long use in several disciplines such as meteorology and civil engineering, the method has only recently been applied to seismological problems [*Alterman and Karal,* 1968; *Alsop,* 1970]. In particular, elasticity problems have been extensively treated in mechanical and civil engineering, and useful techniques, such as the finite-element method [*Zienkiewicz and Cheung,* 1967], have been developed. These problems deal mainly with statics or eigenvibrations, however, and thus are basically concerned with solutions to an elliptic rather than hyperbolic differential equation. I found the simple finite-difference formalism discussed below to be sufficient for the computations in this paper.

Equations of motion. Basically, the medium is replaced by a gridwork of arbitrary spacing, such as in Figure 2. The five points at time level p constitute a computational 'star.' The Laplacian at a given time and spatial node point can be written in terms of the star displacements as (see Appendix 1)

$$(\nabla^2 v)_{m,n,p} \cong \frac{1}{(\Delta x)^2}\{v_{m+1,n}{}^p - 2v_{m,n}{}^p + v_{m-1,n}{}^p\} + 2\left\{\frac{v_{m,n+1}{}^p}{h_2(h_1+h_2)} - \frac{v_{m,n}{}^p}{h_1 h_2} + \frac{v_{m,n-1}{}^p}{h_1(h_1+h_2)}\right\} \quad (6)$$

where h_1, h_2 are consecutive z spacings. Note that three indices are required to specify the location of the grid point in the (x, z, t)-space: m, n are spatial indices, and p is a time index. Also notice that the Laplacian is evaluated at the time p. This, as explained below, leads to a requirement between the spatial and time increments that is necessary for stability, but it also leads to a simple solution to the equation of motion. Note further the uneven spacing in the z direction. This spacing takes advantage of the decay with depth of the Love-wave displacements and thus results in less computer storage. In practice, the z scaling started in the lower material, as this made the interface condition easier to compute.

By approximating the time derivative in the same way as the Laplacian, the equation of motion in medium i at the point (m, n, p) can be written as

$$v_{m,n}{}^{p+1} = 2v_{m,n}{}^p - v_{m,n}{}^{p-1} + \Delta t^2 \beta_i{}^2 (\nabla^2 v_i)_{m,n,p} \quad (7)$$

where the first two terms on the right-hand side arise from the time-derivative approximation. In this form the efficacy of writing the Laplacian at time p is seen: given v at two previous time points and several adjacent spatial points, the displacement at a new time $p + 1$ can be computed by a simple formula. A disadvantage, however, is that for stability of the computations the time increment cannot be chosen independently of the spatial increment. This limitation can be removed if the Laplacian is written as

$$(\nabla^2 v)_{m,n}{}^p = \tfrac{1}{4}(\delta^2 v)_{m,n}{}^{p+1} + \tfrac{1}{2}(\delta^2 v)_{m,n}{}^p + \tfrac{1}{4}(\delta^2 v)_{m,n}{}^{p-1}$$

where $(\delta^2 v)_{m,n}{}^j$ is symbolic for the standard

difference approximation as given in (6) but evaluated at time point j [*Richtmeyer and Morton,* 1967]. This leads to a coupled system of equations for the displacement at the new time $p + 1$, and thus the computation time required to go from times p to $p + 1$ is longer than in the simple forward-step scheme. The advantage of the implicit scheme is that large time increments can be used, and thus the total computation time may be smaller than in the explicit scheme. If, however, the displacement field is changing fairly rapidly, the use of a large t, although stable, will lead to inaccuracies in the approximation of the time derivative, and then the advantage of the implicit scheme will be lost. For this reason and for convenience, the simple forward-step method was used in the computations discussed in this paper.

Boundary conditions. The manner in which an interface condition is approximated is, as far as the author knows, guided mainly by experience. It is difficult to predict a priori whether or not a given technique will lead to accurate, stable results. For instance, a method that works well for one type of boundary may be quite poor in a different application. As an example, the method described below for the interface boundary condition gives better results for Love waves, traveling essentially horizontally, than for *SH* waves at vertical incidence to the boundary. A similar experience for *P-SV* motion is described by *Alterman and Rotenberg* [1969].

If the z index of the free surface is 2, the stress-free boundary condition (2) can be approximated by the 'mirror-image' condition

$$v_{m,1}{}^{p} = v_{m,3}{}^{p} \tag{8}$$

where the z spacing is assumed to be constant in this region. This equation is derived by creating a fictitious layer at $n - 1$ and writing a centered difference approximation to $\partial v/\partial z$. The advantages of this are that the approximation of the derivative is of second order and that the equation of motion can be written at $n = 2$ (the real free surface).

Of the several possible ways of treating the interface boundary condition, the simplest will be discussed below. It was found to be sufficient for the computations in this paper. More detail on this and other techniques can be found in *Boore* [1969]. Consider Figure 3, in which a portion of the spatial gridwork in the vicinity of the boundary is illustrated. Because the interface cuts the grid lines at an angle, the Laplacian at certain grid points near the interface cannot be approximated by a regular star wholly contained within one medium. The Laplacian at these 'funny points' can be written in terms of an irregular star (Appendix 1). This star will involve displacements at actual grid points and at 'curve points' defined by intersections of the interface with the grid lines. Thus in Figure 3 point A is a funny point, and point D is one of the two curve points that would be used in the irregular star placed at A. Assuming that displacements are known at all grid points, funny points, and curve points at times p, $p - 1$ the difference equation can be used to generate new displacements at time $p + 1$ at all points but the curve points. The new curve-point values are obtained by difference approximations to the interface conditions (3) and (4). First a normal is constructed at D. If the displacements at the normal and grid-line intersections C, C′ are known then, equation (3) can be approximated:

$$\mu_1(v_D{}^{p+1} - v_C{}^{p+1})/DC = \mu_2(v_{C'}{}^{p+1} - v_D{}^{p+1})/DC' \tag{9}$$

where DC, DC' are the lengths along the normal from C, C' to D. From this equation the new displacement at D is found. The displacement at C (and similarly for C') is approximated by linear interpolation between A and B. The

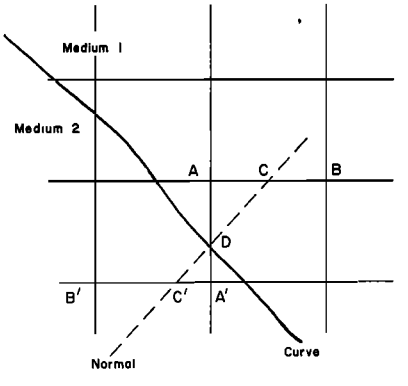

Fig. 3. A portion of the spatial grid near a curved interface showing the location of the normal to the boundary and the funny-points and curve-points discussed in the text.

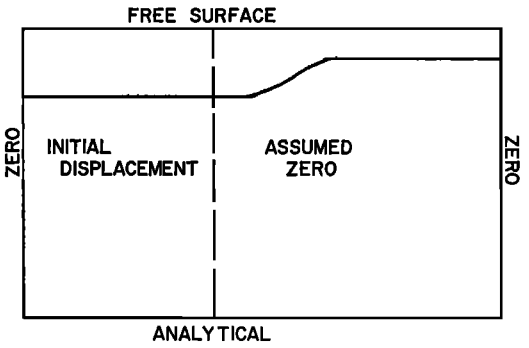

Fig. 4. A schematic diagram summarizing both the boundary conditions used at the artificial interfaces and the location of the initial displacements.

continuity condition (4) was used in the derivation of (9). A basic assumption in the above derivation is that the new curve-point displacements must satisfy the continuity of displacement and stress but are not explicity required to satisfy the equation of motion. The curve points are influenced by the equation of motion indirectly since the new displacements may be thought of as weighted averages of nearby displacements that are required to satisfy the wave equation. If the displacements on a given side of the boundary are smoothly and slowly varying with respect to the grid spacing, this simplification should be of little consequence in the accuracy of the computations.

Although the two interfaces described above are the only real interfaces in the problem, the limitations of finite computer storage force the introduction of fictitious boundaries on the sides and bottom (Figure 4). For reasons explained below, the displacement along the left side was set to zero for all times. The displacements along the bottom were either given exactly at each time step in problems possessing analytical solutions, or were approximated at each time by values appropriate to the incident Love wave. In the latter case, spurious disturbances from this boundary could lead to contamination of the surface values if the bottom was not deep enough. Experiments with several different depths-to-bottom showed this effect to be negligible in the examples presented. The right-hand boundary was always far enough removed that, for the length of time used, the wave disturbance did not have a chance to cause significant reflections from this boundary.

Initial conditions. As mentioned earlier, the initial displacements are taken to correspond to Love waves propagating along a layer of appropriate thickness. Instead of giving displacement and velocity at $t = 0$, we give theoretical displacements throughout the grid for times $t = 0$ and Δt $(p = 0, 1)$. The theoretical displacements are calculated by a Fourier synthesis of the component eigenfunctions such that the surface displacement at $t = 0$ has the form of a Ricker wavelet [*Ricker,* 1945]. Details of the synthesis are given in Appendix 2. The dimensions of the grid are such that the input displacement is, for all practical purposes, wholly contained within the region bounded by the left-hand fictitious boundary and the region of sloping interface. Thus we set to zero displacements outside this region (Figure 4). The containment on the left side is not necessary, for we can compute the theoretical displacement for the incoming wave along the left boundary at any time. Since, however, this requires either a Fourier synthesis over wave number at each depth and time point, which is expensive, or the initial computation and storage of displacements synthesized over frequency at each depth point, which is space consuming, the containment of the initial displacements within the described area was considered to be the most practical procedure. This is an illustration of the storage-space, computation-time tradeoff often encountered in finite-difference problems.

It should be emphasized at this point that the only particularization to Love-wave displacement has been in the specification of the initial conditions. The equations of motion and boundary conditions are completely general. Except for possible fictitious boundary disturbances, the difference scheme should give the total wave solution to the formulated problem as the initial disturbance propagates into the heterogeneous medium.

Stability and accuracy. The influence of the system as a whole (difference equations, interface equations, and initial displacements) should be considered in evaluating the stability and accuracy of a difference scheme. The difficulty of doing this in practice forces one to look at each component separately in the hope

that by so doing one can get a general idea of the total behavior.

It is quite easy to show [*Boore*, 1969] that the truncation error inherent in (6) is such that in the limit Δx, $\Delta t \rightarrow 0$, the difference equation approaches the differential equation as order Δx^2, Δt^2. A standard stability analysis [*O'Brien et al.*, 1950] indicates the difference equation is unstable unless

$$(\beta \Delta t / \Delta h)^2 \leq \tfrac{1}{2} \tag{10}$$

where Δh is the minimum spatial grid spacing and β is the maximum shear velocity. This restriction is not severe but does require a smaller time step than seems necessary. As discussed earlier, there are several ways of writing the difference equations so that unconditional stability is achieved, but the resulting equations are implicit and their solution is not as convenient as the forward time-step method used here.

As previously mentioned, the influence of the interface condition on the accuracy and stability is difficult to determine a priori, and an empirical approach must be taken. Several observations can be made, however. The approximation of (3) uses single-sided differences, which are of order Δz rather than $(\Delta z)^2$ as in the equations of motion and free surface condition. Furthermore, in contrast to the approximation of (2), the material near the interface is in effect not required to satisfy the equations of motion since these equations are not explicitly used in determining the displacement at curve points for time $p + 1$. Another problem with the approach taken for the interface conditions is that the use of an irregular star at funny points implies that locally the stability condition (10) may not be satisfied. This disadvantage is partially offset, however, since in such a case material closer than usual to the boundary is required to satisfy the equation of motion, and thus the determination of the boundary displacements as weighted averages of nearby displacements is more accurate. In practice, instabilities did not often arise from the local violation of the stability condition.

The effect of the initial conditions is not as difficult to determine. Here we can appeal to concepts of filtering and sampling theory [*Hamming*, 1962]. To avoid aliasing, the initial displacement should have no spatial frequencies greater than $\pi/\Delta x$. To assure that the difference approximation is an accurate representation of the actual derivative, the spatial frequencies should be even lower than this. For example, the difference approximation to the second derivative of a function possessing spatial frequencies as high as (3/10) $\pi/\Delta x$ may be in error by as much as 8%.

Discussion. In summary, the solution to the formulated problem follows from several steps. First, the initial displacements at two times are generated. Next, the grid is swept by the difference equation (7) to generate displacements at the next time step. Note that because many grid values are initially zero, only a steadily increasing portion of the entire grid need be swept at each time iteration. Following this the new curve and fictitious point values are found from (8) and (9), and the bottom boundary displacements are given by analytic values. The process is recycled as many times as desired, with printer-plot 'snapshots' of the motion generated at desired times. Displacement values from 'seismometers' located at arbitrary positions in the medium are stored at predetermined time intervals and after completion of the time cycles are punched on cards to be used in subsequent processing, such as phase-velocity determination and transfer ratio computations. It is interesting to note that although the initial displacement must be rather pulse-like because of the limitations of storage space, the effect of the heterogeneity on the time-domain representation of a more realistic, dispersed wave train can be simulated by using the pulse results to derive the transfer spectrum between any two seismometer locations.

Typically, a grid 300 by 60 was used with 300 time iterations. The structure of (7) is such that only two rather than three spatial grids need to stored. Running time, exclusive of the generation of initial displacements but including output, was approximately 8 min on an IBM 360/65. Program optimization was not attempted. The initial displacements were generated in a separate program and kept on permanent file. Using a Fast Fourier Transform, the synthesis of the Love displacements at a given depth and time required about 0.3 seconds for 512 wave number points. The amplitude spectrum of the initial displacement was such that approximately 34 grid points

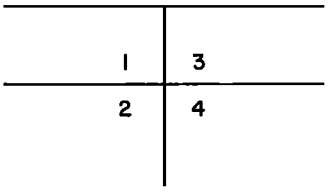

$$\text{I.} \quad \frac{1}{\beta_1^2} - \frac{1}{\beta_2^2} = \frac{1}{\beta_3^2} - \frac{1}{\beta_4^2}$$

$$\text{II.} \quad \frac{\mu_1}{\mu_2} = \frac{\mu_3}{\mu_4}$$

Fig. 5. The geometry and media labels for four materials joining along a vertical interface. If the two conditions at the bottom are satisfied, an analytic solution to the problem of an incident Love wave can be found.

were contained within the dominant wavelength.

Application to Problems with Known Solution

Vertical-boundary problem. As the first illustration, we shall apply the technique to a problem first discussed by *Higuchi* [1932] and more recently by *Sato* [1961] and *Alsop* [1966]. In this problem (Figure 5) a Love wave on a combination of layer and half-space is incident to another layer and half-space combination separated from the first by a vertical boundary. If the elastic constants of the four materials are not chosen independently but satisfy the two relationships shown in Figure 5, the complete wave solution to this problem can be represented by an incident, reflected, and transmitted Love wave of a given mode.

Calculated surface displacements generated by the difference scheme are shown in Figure 6 for different instances of time. In this problem, elastic constants were chosen such that the reflected wave would be prominent. The constants chosen are not intended to model a realistic boundary. The initially symmetric Ricker wavelet is distorted by dispersion, is reflected, and is transmitted. The slope discontinuities at the vertical boundary, most obvious at times $t = 70$ and $t = 84$, are necessary consequences of the continuity of the stress component σ_{yz}. Another illustration of the same calculations is given in Figure 7, where printer-plot contours of displacement on a vertical profile are shown for different times. The top edge of each plot corresponds to the free surface. The variable grid spacing with depth produces a distorted picture of the vertical variation. The horizontal interface is drawn in the last plot ($t = 112$) and the vertical interface is given by the vertical line. Each plot can be viewed as a contour map of the displacements at each grid point for a certain instant of time, in which the area between every other contour is indicated by a given symbol. These plots are only intended to give a qualitative picture of the displacement variation in space and time, and thus the actual values of the contours are irrelevant.

Theoretical displacements based on a Fourier synthesis of the eigenfunction solutions are indistinguishable from the computed displacements illustrated in Figure 6. More details concerning this synthesis and the treatment of the interfaces (especially the four-intersection point) may be found in *Boore* [1969].

Dispersion problem. The example above indicated that the method works, but the results are not particularly useful. Of more interest is the simulation of a phase-velocity-measurement experiment. As a simple example of this and as a preliminary to the next section, the incident Love wave was allowed to propagate on the initial layer and half-space combination. Figure 8 shows seismograms for several locali-

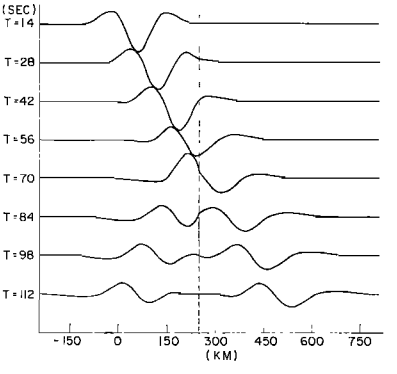

Fig. 6. The surface displacements at different instants of time for the problem indicated in Figure 5. The location of the vertical interface is given by the dashed line. The various elastic and geometric parameters, $\beta_1 = 3.85$, $\rho_1 = 3.0$, $\beta_2 = 4.75$, $\rho_2 = 3.65$, $\beta_3 = 4.23$, $\rho_3 = 7.44$, $\beta_4 = 5.53$, $\rho_4 = 8.07$, $H = 35.0$, were chosen such that a large reflected wave would be present. The units of β and ρ are km/sec and g/cm^3.

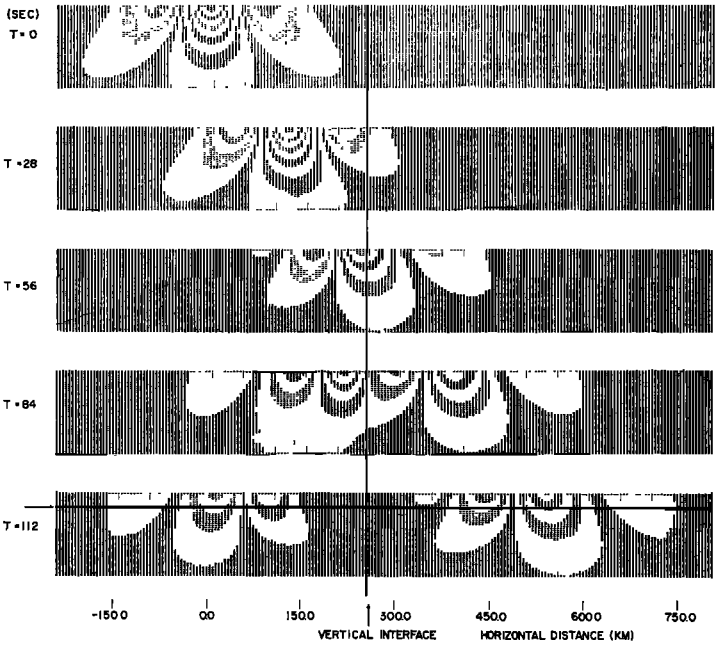

Fig. 7. Computer-generated contour plots of the spatial distribution of Love-wave displacements at different instants of time for the problem illustrated in Figure 5. The results here are derived from the same experiment as those in Figure 6. An explanation of the contours is given in the text.

ties along the surface. In this figure the distortion of the initially symmetric pulse is quite obvious. By taking the Fourier transforms of these seismograms, the phase velocities shown in Figure 9 were calculated by the standard least-squares technique (adapted to in-line stations). Due to the premature termination of the fourth seismogram, only three sites were used in this computation. Phase velocities for a run with a thinner layer (represented by only three grid points) are also included. In spite of the relative closeness of the stations, the computed phase velocities are in excellent agreement with the theory. This was expected since the seismograms themselves agreed with

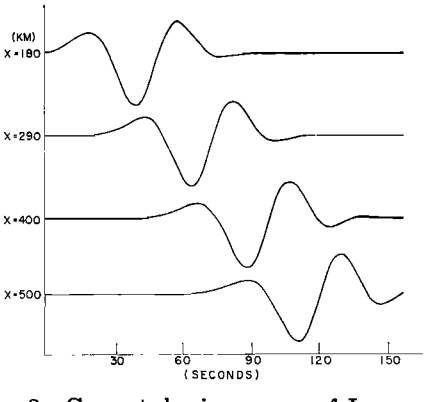

Fig. 8. Computed seismograms of Love waves for various sites along the surface of a layer of uniform thickness over a half-space. In this experiment $\Delta x = 5$ km and $\Delta t = 0.7$ sec. Theoretical wave forms are virtually identical to these computed wave forms.

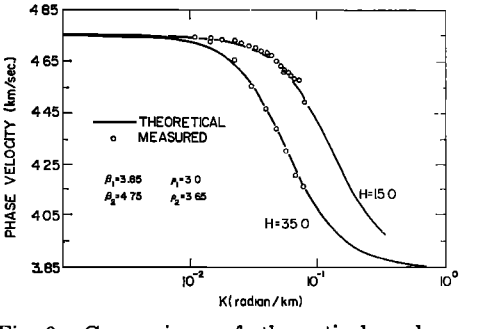

Fig. 9. Comparison of theoretical and computed phase velocities, plotted against wave number. The measured values were derived from the phase spectrum of seismograms such as in Figure 8.

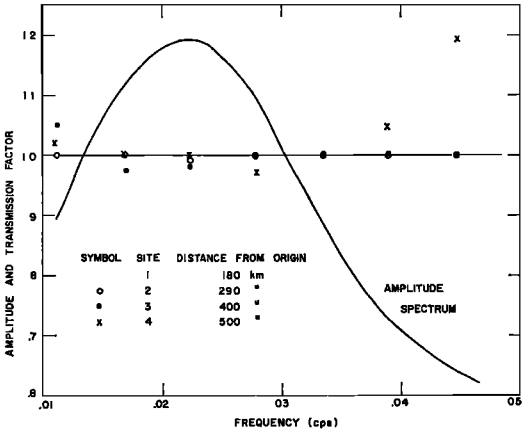

Fig. 10. The amplitude spectrum (arbitrary units) of the initial transient, along with the measured transmission factor for the model of layer and half-space used in Figures 8 and 9 (with $H = 35$ km). Theoretically the transmission factor should be unity. The divergence at higher frequencies for site 4 is a truncation effect, since not enough of the time series at this site was generated.

the theoretical displacements. For wave numbers on either side of the range illustrated, however, the phase-velocity agreement was not good. For the larger wave numbers this was undoubtedly due to the relatively small amount of power contained in the initial displacements. The scatter at low wave numbers is attributable both to insufficient power and to insufficient station spacing. The amplitude spectrum of the initial wavelet is shown in Figure 10, along with the measured transmission factors for the thick-layer calculations. The transmission factors, defined as the amplitude spectrum at a given station normalized by the spectrum at the first station encountered, can be a sensitive indicator of subsurface structural variations.

Of interest is whether the inaccuracies in the computations are steadily increasing with time, or whether they tend to damp out. The extreme case of instability, of course, is easy to recognize, but a gradual loss of accuracy is not. To study this, the Fourier transforms of the surface displacements at different times were compared with theoretical wave number spectra. The error was investigated in the wave number rather than the frequency domain since the displacements throughout the grid at any fixed time represent the same number of algebraic manipulations. This is opposed to the time series at a given node point, in which each value represents a different number of computations. Since, however, the error propagates as a wave, the ideal would be to study the error spectrum in the frequency and wave-number space.

The amplitude error is defined as the percentage of difference between the computed and theoretical wave number spectral amplitudes:

$$\text{error } (k, t) \equiv 100 \cdot \left\{ \frac{|V_T(k, t)| - |V_C(k, t)|}{|V_T(k, t)|} \right\}$$

where the time and wave-number dependence has been indicated. The amplitude errors for the Love-wave computations with a 15-km layer (the layer being represented by only two grid points exclusive of the free surface and interface) are given as a function of time and wave number in the last three columns of Table 1*a*. The first column contains the wave number; the second column contains, for reference, the theoretical amplitude for each wave number. This table shows that the absolute difference in amplitude is small, that the relative error (e.g., error at $t = 84$ compared to that at $t = 42$) increases with time, and that the computed amplitudes are consistently lower than the theoretical amplitudes. The aberrant behavior at $k = 0.07363$ in the relative increase of error with time is probably related to the small amount of power in the initial displacements at this wave number.

The phase information is contained in Table 1*b*, where the error measure is defined by the relation

TABLE 1a. Error in Amplitude as a Function of Wave Number and Time

k	Theoretical Amplitude	$t = 42$	84	126
0.01227	0.15	−0.43	−1.15	−1.90
0.02454	0.35	−1.64	−2.21	−2.86
0.03682	0.30	−2.36	−3.36	−4.49
0.04909	0.15	−2.54	−4.11	−4.54
0.06136	0.04	−2.56	−2.80	−3.96
0.07363	0.008	−1.80	−8.70	−0.85

Note:
See text for explanation.

$$\delta\phi_{ij} \equiv 100 \cdot \left\{ \frac{[\phi_i^t - \phi_j^t] - [\phi_i^c - \phi_j^c]}{[\phi_i^t - \phi_j^t]} \right\}$$

where ϕ_i^t, ϕ_i^c are the theoretical and calculated phases (with phase integers added when necessary to account for the multivaluedness of the measured phase spectra) at time $t = t_i$ (42, 84, and 126 sec). $\delta\phi_{ij}$ expresses the relative error in the phase difference between two sites and hence is equivalent to the error expected in the phase-velocity calculations. As in the case of amplitudes, Table 1*b* shows that the error again seems to be biased (corresponding to an overestimation of phase velocity) but it is not obviously increasing.

The errors indicated in Tables 1*a* and 1*b*, based on wave-number domain calculations, and the errors implied by the frequency-domain results in Figures 9 and 10, indicate that the Love-wave finite-difference calculations are of sufficient accuracy to warrant an investigation of a more complicated problem. The remainder of this paper will be a discussion of such a problem.

Application to Sloping Layer Problem

The geometry and elastic constants for the problem of an idealized ocean–continent boundary, with a crust of 15-km thickness increasing to one of 35-km thickness over a distance of 120 km, are illustrated in Figure 11. A water layer is not included. In order to study the effect on measured phase velocities of two-way propagation across a given station pair, computations were performed with the initial Love-wave incident from both directions. The initial pulse was identical to that used in the flat-layer dispersion experiment described above. Six

TABLE 1*b*. Error in Phase as a Function of Wave Number and Time

k	$\delta\phi_{12}$	$\delta\phi_{13}$	$\delta\phi_{23}$
0.01227	−0.02	−0.22	−0.41
0.02454	−0.21	−0.10	0.00
0.03682	−0.32	−0.31	−0.30
0.04909	−0.26	−0.22	−0.19
0.06136	−0.32	−0.35	−0.37
0.07363	−0 26	0.00	0.26

Note:
See text for explanation.

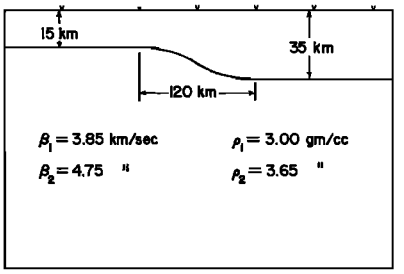

Fig. 11. Schematic diagram of the nonuniform wave guide problem. The *v*'s at the top represent possible seismometer sites (see text). Grid spacings of $\Delta x = 5$ km and $\Delta t = 0.7$ km were used.

stations, at each of which a time series was generated, were arranged in the following manner with respect to the transition region: one station was placed on the near side of the transition zone as seen from the incident wave, stations were put on either end of the zone, one was placed in the middle, and two were placed on the far side of the zone. Thus in Figure 11 the *v*'s represent seismometer sites 1 through 6 for a wave incident from the left. The numbering always starts with the first site encountered. Thus the same geometrical location will have two site numbers depending on the direction of the incident wave.

In subsequent discussion the terms *updip* and *downdip* are used to indicate the direction of the incident wave; downdip represents propagation from the ocean to continent and updip is from continent to ocean. Phase velocities calculated for the following station locations will be illustrated: thin side (1–2) and thick side (4–5), both of which are underlain by a flat Moho; thin–middle (2–3), middle–thick (3–4), and thin–thick (2–3–4), situated over the region of the sloping Moho. The station numbers in parentheses are appropriate to downdip propagation. Furthermore, for each direction of incidence two station pairs were used on the far side of the transition region (4–5; 5–6). Doing this gives a qualitative check on the solution, for the farther the wave gets from the boundary, the closer the measured phase velocity should approach the theoretical dispersion for a flat layer of the appropriate thickness covering a half-space.

Figure 12 contains two-way phase velocities measured over regions with a flat Moho. For

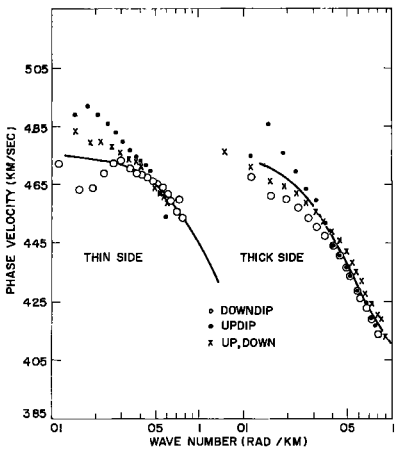

Fig. 12. Measured phase velocities over flat portions of the wave guide. The solid lines are the appropriate theoretical values. The graphs have been horizontally separated for clarity. The crosses refer to updip propagation in the left-hand graph and downdip in the right-hand graph.

clarity the thin side and thick side graphs have been separated. We see that the measured dispersion is anisotropic in that it depends on the direction in which the wave is traveling, and that the anisotropy tends to disappear for shorter wavelengths. This dependence on wavelength agrees with intuitive expectations. since for stations removed from the boundary it is only the longer wavelengths that should be 'seeing' the transition region. In line with this, the phase velocities calculated from the station pair most distant from the transition region (given by crosses in Figure 12) appear to be approaching the theoretical curve, as we would expect. The critical distance is on the order of one wavelength; for stations farther from the transition than a wavelength, the effect will be small. Even if the measuring array is closer than this to the transition zone, a reasonable approximation to the local structure can be obtained by basing interpretations on an average of down- and updip phase velocities. A further observation is that the downdip propagation gives, in this model, consistently lower phase velocities than does updip propagation.

The phase velocities measured over the transition region show similar features (Figure 13): the phase velocity is strongly anisotropic, and the downdip propagation velocities are consistently lower than are the updip velocities. Here, however, the anistropy is greatest in the middle range of wave numbers. The phase velocities for smaller wave numbers are isotropic and biased. Also of interest is that the velocity difference between up- and downdip propagation can exceed the difference due to structure alone, and that downdip propagation is less perturbed than is updip propagation. Here an average of up- and downdip propagation is not as effective in removing the perturbations as it was when the measurement stations were removed from the transition region.

Although the phase velocity contains all the information that exists in the phase spectrum, it is instructive to look at the group delays separately. The group delays for each site were computed from the definition

$$\tau_g(x, \omega) = [d\phi(x, \omega)/d\omega]$$

by approximating the derivative by a two-sided difference. The theoretical group delays were found for each frequency by approximating the boundary by a series of flat layers and accumulating the group delays for each layer. This theoretical approach is equivalent to a first-order WKBJ solution to the problem. The resulting difference between the theoretical and measured group delays is plotted against frequency in Figure 14 for both up- and downdip propagation. As might have been expected from the behavior of the phase-velocity curves, the

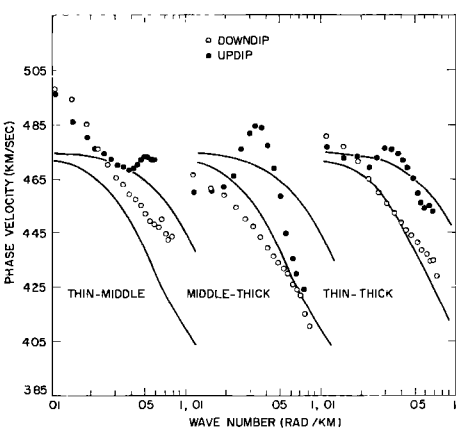

Fig. 13. Phase velocities measured over the region of nonuniform thickness. The solid lines are theoretical values for the thin- and thick-layer models and are for reference only.

transition zone contributes the most perturbation. The similar character of the delay at sites 4, 5, and 6 indicates that passage through the transition zone has caused a relative advance of up to 2.0 sec at the low frequencies and delay of less than 2.0 sec at the high frequencies in the case of updip propagation. Downdip propagation, again as in the case of the phase velocity, is not as affected by the transition zone. The implications of these results are that the standard practice of deriving an effective group velocity for a composite path by using an inverse average of the component parts is justified, and that measurements of group velocities between an epicenter and station will be negligibly biased by the effect of the ocean–continent margin. This latter implication is especially true since the epicenter and station locations are usually such that the sense of propagation will be downdip (from the ocean to the continent).

Up to this point only the phase information of the computed seismograms has been utilized, but the amplitude information is also useful. A convenient way of presenting this information is in terms of transmission factors (defined earlier) at the various stations (Figure 15). Note that the curves for sites 4, 5, and 6, all located on the far side of the transition region, have similar shape and tend to approach the theoretical curve with increasing distance from the zone. This theoretical curve is based on the simple assumption that all the energy flow in the incident wave is somehow transferred into the wave guide represented by the layer and half-space combination on the far side of the transition zone. No reflected energy or mode conversions are taken into account. Several other approximate theories, all of which take partial reflections into account, give theoretical curves similar to the ones in Figure 15 [*Boore*, 1969]. The theories include a hybrid taken from *Knopoff and Mal* [1967] and *Alsop* [1966], and a theory developed from analogy with a transmission-line problem. I should mention that although at a large distance from the transition region the theoretical and calculated transmission factors are similar, this similarity breaks down drastically in the vicinity of the region. This is true for both the predicted phase velocity and the transmission factors. Since the approximate theories take no account of scat-

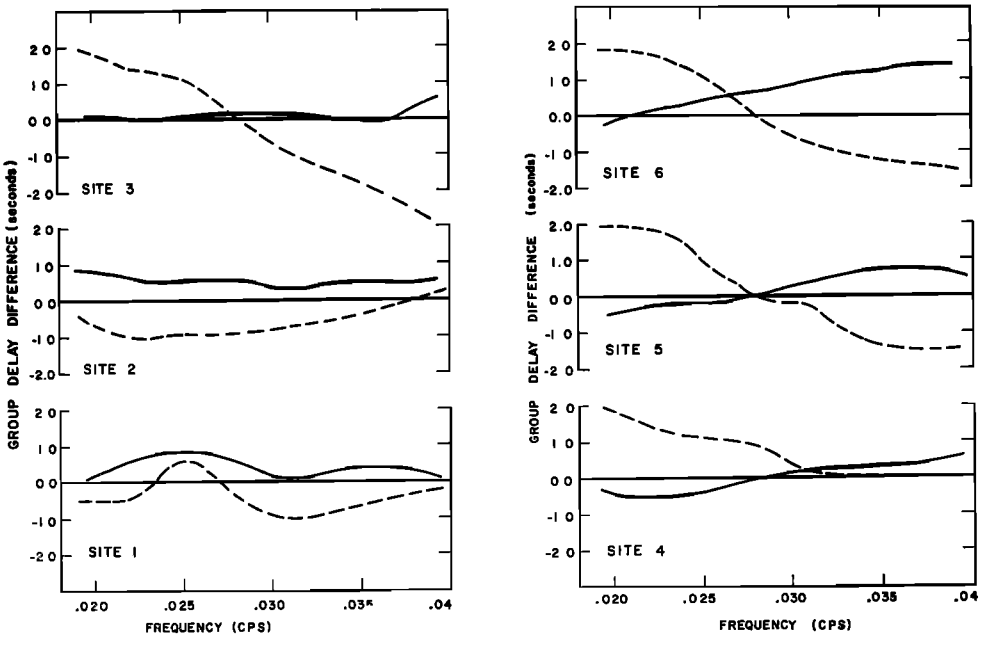

Figs. 14. The difference between theoretical and measured group delays versus frequency for the various sites. The solid lines are for downdip propagation and the dashed lines for updip.

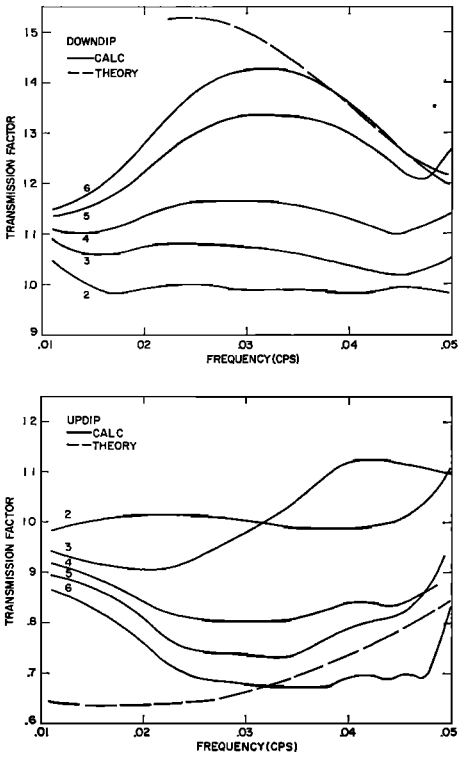

Fig. 15. Transmission factors.

tered fields, which require other waves like leaking modes, this leads to the conclusion that such waves must be an important component of the total disturbance in the transition region. I expect that such modes become increasingly less important as the slope of the interface is decreased.

In problems such as this that possess no analytical answer, the correctness of the results must be judged both on the basis of experience with simpler problems and the qualitative behavior of the solution. As the previous section indicated, the finite-difference technique gave excellent results for simple models, but in neither of the examples presented was the curved-boundary approximation used. We must allow for the possibility that the method of treating the interface conditions across the curved region leads to fictitious sources that give rise to the peculiar behavior of the phase velocities and transmission factors. The evidence against this possibility are several: (1) an updip run with $\Delta x = 3.0$ km rather than 5.0 km gave virtually identical results; (2) using a higher order generalization of the interface-condition approximation gave similar results; (3) the phase velocities from an updip run in which the layer decreased in thickness from 35 km to 25 km rather than 15 km showed similar perturbations, but of smaller magnitude (Figures 16 and 17); (4) application of the curved boundary approximation to the problem of an *SH* wave vertically incident from below on a layer with a bump in it gave results that agreed, after application of a suitable exponential window, with those computed via the technique of *Aki and Larner* [1969].

From the tests (1), (2), and (4) above, I estimate that the computed phase velocities are accurate to within at least 3% and usually 1.5% in the period range illustrated, with the possible exception of some of the values on either end of the range where the small amount of power, truncation, or large wavelength relative to the station spacing can reduce this accuracy. The amplitude-transmission factors are good to within 5% over most of the period range. A more complete discussion of the tests above and the corresponding accuracy is given in *Boore* [1969].

It is tempting to point out that the tendency for updip propagation to give high phase ve-

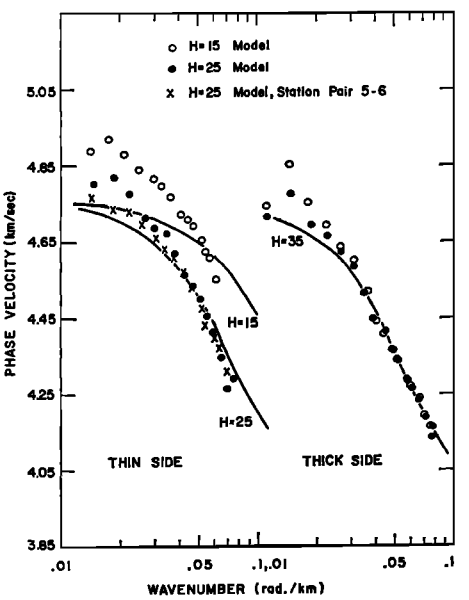

Fig. 16. Comparison of measured updip phase velocities over flat portions of the interface for models in which the layer thins to 15 km (previous case) and 25 km.

locities is expected if one thinks of the apparent surface velocity of a traveling wave bouncing between the free surface and the interface. This result, however, is opposite to that found by *Pec* [1967] for Love waves propagating in a wedge. Pec determined the local phase velocity by requiring constructive interference, and thus considered both the wavelength and ray path of the bouncing wave. It is not clear that Pec's analysis is applicable here, for the comparability of the incident wavelength and the horizontal extent of the transition zone means that the wave in effect does not see a wedge.

Discussion

In summary, the finite-difference method appears to be a useful tool in dealing with fairly complex structures. The method is most useful in the near-field region of sources, where the sources can be either real or, as in this paper, effective sources introduced by complexities along the travel path. In the latter case we use analytic results to describe the wave motion between the real, physical source (in this paper the source is at $x = -\infty$) and the region of inhomogeneity, and we use the finite-difference scheme to propagate the disturbance through this region. Application to the problem of Love waves propagating across an idealized ocean–continent boundary indicates that significant perturbations of both the phase and amplitude spectrums can occur in the vicinity of the transition region, and that these perturbations become less important at a distance from the boundary. In particular, the behavior at a distance justifies the well-established method of calculating effective group velocities by means of inverse averages of regional group velocities, and also indicates a simple correction for the effect of the ocean–continent boundary that can be applied to calculations of earthquake-source mechanisms based on the method of amplitude equalization. The behavior of the amplitude and phase in the transition region indicates that observable effects should exist for Love waves propagating across structural complexities within the continent, and this suggests a tool for the study of these complexities.

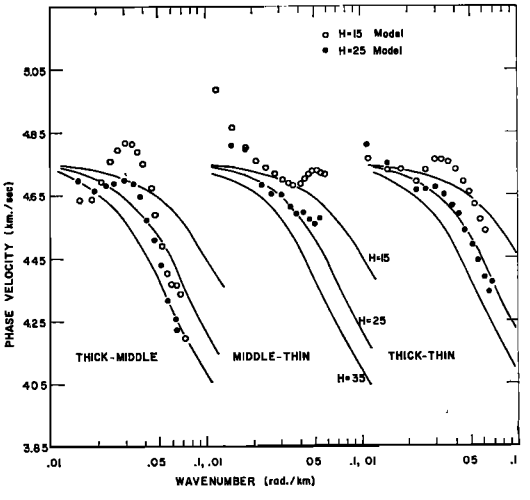

Fig. 17. Comparison of measured updip phase velocities over the transition zone for the two models mentioned in Figure 16.

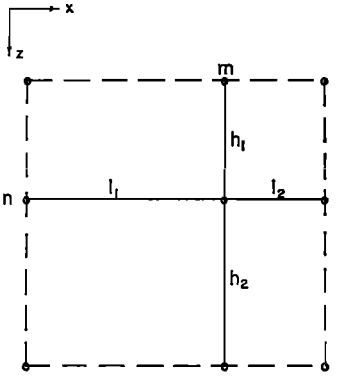

Fig. 18. Lattice used in deriving a finite difference approximation to the Laplacian.

Application to problems involving inhomogeneous, inelastic materials should be possible without significant increases in either computation time or storage space. Rayleigh wave and *P-SV* problems can be handled in a similar fashion, but at cost of approximately twice as much time and space. Application of the finite-difference method to realistic three-dimensional problems requires an order of magnitude more time and space and therefore is not practical at the present time except under extraordinary circumstances.

Appendix 1. Finite Difference Approximation to the Laplacian

Consider the irregular star in Figure 18. Diagonal points are included so that an approximation to the mixed derivative

$$\partial^2 y/\partial x\,\partial z$$

can also be derived if desired. Such a derivative occurs in the general vector elastic equations but will not be evaluated here. We fit a two-dimensional Lagrange polynomial surface to the nine points and then differentiate this function to obtain the approximation to the actual derivatives. Such a polynomial can be represented by

$$y_p(x, z) = \sum_{i=m-1}^{m+1} \sum_{j=n-1}^{n+1} \gamma_{ij} y_{ij} \qquad \text{(A1)}$$

where y_{ij} is the known value of y at $x = x_i$, $z = z_j$, and γ_{ij} are functions of (x, z) given by

$$\gamma_{ij}(x, z) = [P_{ij}(x, z)/P_{ij}(x_i, z_j)] \qquad \text{(A2)}$$

where

$$P_{ij}(x, z) \equiv \prod_{\substack{k=m-1 \\ k\neq i}}^{m+1} \prod_{\substack{l=n-1 \\ l\neq j}}^{n+1} (x - x_k)(z - z_l)$$

the basis of the construction is that $y_p(x_i, z_j) = y_{ij}$. The polynomial y_p is, of course, only an approximation to the actual function y, but we assume that the actual function is smooth enough so that $y_p(x, z) = y(x, z)$ in the local region around x_m, z_n. Taking the second derivatives of y_p with respect to x and z, and evaluating the result at $x = x_m$, $z = z_n$ yields the desired expression for the finite difference approximation of the Laplacian:

$$\begin{aligned}(\nabla^2 y)_{x_m, z_n} = {} & \frac{2}{l_1(l_1 + l_2)}\, y_{m-1,n} \\ & - \frac{2}{l_1 l_2}\, y_{m,n} + \frac{2}{l_2(l_1 + l_2)}\, y_{m+1,n} \\ & + \frac{2}{h_1(h_1 + h_2)}\, y_{m,n-1} - \frac{2}{h_1 h_2}\, y_{m,n} \\ & + \frac{2}{h_2(h_1 + h_2)}\, y_{m,n+1} \qquad \text{(A3)}\end{aligned}$$

The four cross terms do not appear.

Appendix 2. Synthesis of Love Displacements Using Fast Fourier Transforms

We are interested in the Love displacement at some point x, z, t when the displacement on the surface at $t = 0$ is given by the function:

$$v(x, 0, 0) = g(x) \qquad \text{(A4)}$$

Let $F(k, z, t)$ be the eigenfunction solution to the source free Love-wave problem where a spatial transform over the x (horizontal) direction has been taken. The time factor will always appear in the form ωt, but from the dispersion relation for the particular problem being considered $\omega = \omega(k)$. Thus k, z, and t can be considered independent variables. The actual evaluation of F for a given k can be done analytically in the simple case of one layer or can be determined numerically using Haskell matrices in more complicated problems.

Thus a general solution of the Love-wave problem in the space-time domain can be determined by adding up eigenfunctions with appropriate weighting factors:

$$v(x, z, t) = \frac{1}{2\pi} \int_{-\infty}^{\infty} A(k) F(k, z, t) e^{ikx}\, dk \qquad \text{(A5)}$$

Expressing $g(x)$ as a Fourier integral and applying (A4) we find

$$g(x) = \frac{1}{2\pi} \int_{-\infty}^{\infty} G(k) e^{ikx}\, dk$$

$$A(k) F(k, 0, 0) = G(k)$$

or

$$A(k) = G(k)/F(k, 0, 0) \qquad \text{(A6)}$$

so finally

$$v(x, z, t) = \frac{1}{2\pi} \int_{-\infty}^{\infty} \frac{G(k)}{F(k, 0, 0)}\, F(k, z, t) e^{ikx}\, dk \qquad \text{(A7)}$$

Our problem now is to evaluate this integral. The reason for integrating over wave number k, as opposed to frequency ω, is that we can use a Fast Fourier Transform (*FFT*) to evaluate v at many values of x at one value of t and z. Thus we can efficiently generate the initial displacements used in the difference technique.

Evaluating (A7) by means of the Fast Fourier Transform is quite straightforward, but some details are worth mentioning. We assume that a subroutine which can do forward and backward transforms of 2^N complex data points is available. Then with the notation

$$(\text{data})_i = \frac{1}{N\Delta x}\, G[(i - 1)\Delta k]\, \frac{F[(i - 1)\Delta k, z, t]}{F[(i - 1)\Delta k, 0, 0]}$$

and $\Delta k = 2\pi/N\Delta x$, we fill the complex input array with $(\text{data})_i$, $i = 1, 2, \cdots, N/2$. Here Δx is the spatial sampling used in the problem. Note the normalization $1/N\Delta x$. This guarantees that (A4) holds when v is evaluated using a *FFT*.

For input points $i = N/2 + 1$ to N we use the following:

$$\text{Re (data)}_i = \text{Re (data)}_{N+2-i}$$

$$\text{Im (data)}_i = -\text{Im (data)}_{N+2-i}$$

This is necessary since the symmetry of the *FFT* assumes that $(\text{data})_i$, $N/2 < i \leq N$ correspond to negative frequency points and because $v(x, z, t)$ is real. Thus the transform of v, $V(k, z, t)$, has the property

$$V(-k, z, t) = V^*(k, z, t)$$

where * indicates a complex conjugate. We now apply the *FFT* to the complex array $(\text{data})_i$ and end up with another complex array $(\text{result})_i$, $i = 1, N$. Here

$$\text{Im (result)}_i \cong 0.0$$

and Re(result)_i contains the answer for which we are looking.

Because of the periodic nature of the finite Fourier transform, some juxtaposition of terms is required if the initial surface displacements are nonzero for $x < 0$. The corresponding displacements will be found at the end rather than the beginning of the array containing the results. This transposition is easy to accomplish, but could be avoided by shifting the x-origin in the beginning such that all initial displacements lie to the right.

Thus with one call to a *FFT* subroutine we have evaluated the integral (A7) at a given z, t, and N values of x.

Acknowledgments. The constant advice and criticism of Keiiti Aki, Ken Larner, and Ralph Wiggins have been very helpful. Besides this valuable dialogue, Professor Aki gave the initial impetus to work on this problem, and Dr. Wiggins supplied several of the auxiliary computer programs.

The research reported here was partially supported by the Advanced Research Projects Agency, monitored by the Air Force Office of Scientific Research under contract AF49(638)-1632 and by the National Science Foundation under grant GA-4039. During part of this work the author was supported by an NSF traineeship.

References

Aki, K., and K. L. Larner, Surface motion of a layered medium having an irregular interface due to incident plane *SH* waves, *J. Geophys. Res., 75*(5), 1970.

Alexander, S. S., Surface-wave propagation in the Western United States, Ph.D. thesis, California Institute of Technology, Pasadena, 1963.

Alsop, L. E., Transmission and reflection of Love waves at a vertical discontinuity, *J. Geophys. Res., 71,* 3969–3984, 1966.

Alsop, L. E., Solution of elastic wave equations by finite-difference methods, *Rev. Geophys.,* in press 1970.

Alterman, Z. S., and F. C. Karal, Jr., Propagation of elastic waves in layered media by finite-difference methods, *Bull. Seismol. Soc. Amer., 58,* 367–398, 1968.

Alterman, Z. S., and A. Rotenberg, Seismic waves in a quarter plane, *Bull. Seismol. Soc. Amer., 59,* 347–368, 1969.

Boore, D. M., Finite-difference solutions to the equation of elastic wave propagation, with application to Love waves over dipping interfaces, Ph.D. thesis, Massachusetts Institute of Technology, Cambridge, 1969.

Ghosh, M. L., On Love waves across the ocean, *Geophys. J. Roy. Astron. Soc., 7,* 350–360, 1962.

Hamming, R. W., *Numerical Methods for Scientists and Engineers,* 411 pp., McGraw-Hill, New York, 1962.

Higuchi, S., On Love dispersion in a complicated surface layer (in Japanese), *Zisin, ser. 1, 4,* 271–276, 1932.

Knopoff, L., and A. K. Mal, Phase velocity of surface waves in the transition zone of continental margins, *J. Geophys. Res., 72,* 1769–1776, 1967.

Kuo, J. T., and G. A. Thompson, Model studies on the effect of a sloping interface on Rayleigh waves, *J. Geophys. Res., 68,* 6187–6197, 1963.

O'Brien, G. G., M. A. Hyman, and S. Kaplan, A study of the numerical solution of partial differential equations, *J. Math. Phys., 29,* 223–251, 1950.

Pec, K., Theoretical dispersion tables for Love waves propagating in a wedge and in a single non-homogeneous layer with a linear velocity gradient, *Publ. Dominion Observ., 35*(1), Ottawa, Canada, 1967.

Richtmeyer, R. D., and K. W. Morton, *Difference Methods for Initial-Value Problems,* 405 pp., Interscience, New York, 1967.

Ricker, N., The computation of output disturbances from amplifiers for true wavelet inputs, *Geophysics, 10,* 207–220, 1945.

Sato, R., Love waves propagated across transitional zone, *Jap. J. Geophysics, 2,* 117–134, 1961.

Zienkiewicz, O. C., and Y. K. Cheung, *The Finite Element Method in Structural and Continuum Mechanics,* 274 pp., McGraw-Hill, London, 1967.

(Received July 14, 1969.)